Impedance-based Detection of Blood Clotting Time

Riya Varma[†], Asish Koruprolu[†], and Drew A. Hall
† Equally credited authors
Department of Electrical and Computer Engineering, University of California San Diego, La Jolla, CA, USA
drewhall@ucsd.edu

Abstract—**This paper investigates the electrical properties of porcine blood, blood clot, and serum samples by measuring their absolute conductivity across frequency. At 1 kHz, the measured conductivity of blood is 0.44 S/m, blood clot is 0.34 S/m, and serum is 1.50 S/m. An impedance marker is identified to measure blood clotting time, demonstrated by varying the concentration of Ca^{2+} added to initiate clotting. The study accounts for blood drying, serum in the measurement chamber, and electrode parasitics. This research provides a foundation for further exploration and validation of the impedance-based approach in measuring blood clotting time and erythrocyte sedimentation rate to improve clinical practice and advance coagulation monitoring.**

Keywords—Blood clotting, impedance measurements, clot detection, clinical applications.

Fig. 1. Image showing a point-of-care sensor to monitor blood clotting time.

I. INTRODUCTION

Monitoring blood clotting time is crucial in various medical contexts as it plays a significant role in diagnosing clotting disorders, guiding surgical interventions, and monitoring anticoagulant therapies [1]. It is a valuable tool for diagnosing bleeding disorders (*e.g.*, hemophilia and von Willebrand disease) and excessive blood clotting disorders (thrombophilia). Thrombophilia poses significant risks if left untreated and can lead to the development of blood clots in arteries and veins. Physicians use blood clotting time to adjust dosages for patients taking blood-thinning medications (*e.g.*, Warfarin or undergoing antiplatelet therapies) to ensure they can undergo surgery and anticipate excessive bleeding and complications in trauma care, among many others [1].

Various commercial central laboratory-based tests exist to measure blood clotting time [2], [3]. Prothrombin time (PT) assesses the time to clot blood through the extrinsic pathway, commonly used for monitoring oral anticoagulant therapy, while activated partial thromboplastin time (aPTT) measures clotting time via the intrinsic pathway, typically employed to monitor heparin therapy. Additional tests, such as Thrombin time (TT) and fibrinogen assay, evaluate different stages of the coagulation cascade. However, these commercially available tests have inherent limitations, often focusing on specific clotting pathways and lacking a comprehensive assessment of clotting dynamics. Moreover, they require specialized equipment, confining their usage to laboratory settings [4], [5]. Point-of-Care (PoC) viscoelastic tests like Thromboelastography (TEG) and Rotational Thromboelastometry (ROTEM) offer alternatives for assessing hemostasis and clot formation [1], but they also have limitations, requiring highly trained technical personnel and their results being susceptible to processing errors [6]. In contrast, microfabricated sensors utilizing resonant structures like thin-film bulk acoustic resonators, magnetoelastic transducers, or piezoelectric quartz crystals [7]–[9] offer the potential for PoC blood coagulation monitoring by measuring blood viscosity through frequency shifts. Several techniques have been explored to detect fibrin formation using optical [10] and ultrasonic [11] transducers, and by observing changes in mechanical [12] and electrical [13], [14] properties of blood, but they often rely on equipment not amenable to miniaturization.
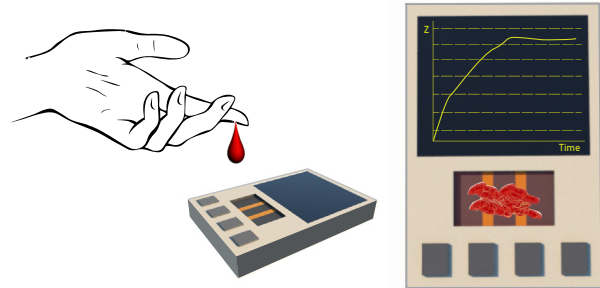
This research introduces an impedance-based clotting time measurement technique that addresses the limitations of current methods and holds the potential to be developed into a low-cost PoC screening system, as shown in Fig. 1. Several authors have proposed different methods for measuring the electrical impedance of blood [15]–[21]. Unlike previously published methods, this comprehensive approach accounts for critical factors such as blood drying, stray capacitance, electrode polarization effects, and the effects of serum ejection in the measurement chamber. By considering these factors collectively, the study provides a more holistic understanding of how the impedance changes when blood clots and measures the erythrocyte sedimentation rate (ESR) and blood clotting time (T_{clot}). This research departs from the relative conductivity measurements and attempts to measure the absolute conductivity of blood and blood clots. This shift is motivated by the significant variability in conductivity values reported for blood clots, aiming to provide more precise assessments of blood clot conductivity.

This technique enables accurate clot identification by utilizing impedance measurements, offering a means to trace the thrombogenic profile of high-risk patients outside specialized clinical laboratories or hospitals. Moreover, the proposed technique requires minimal blood volume, reducing patient discomfort. This research aims to bridge the gap between laboratory-based clotting tests and PoC applications, paving the way for a more accessible and comprehensive approach to blood clotting assessment.
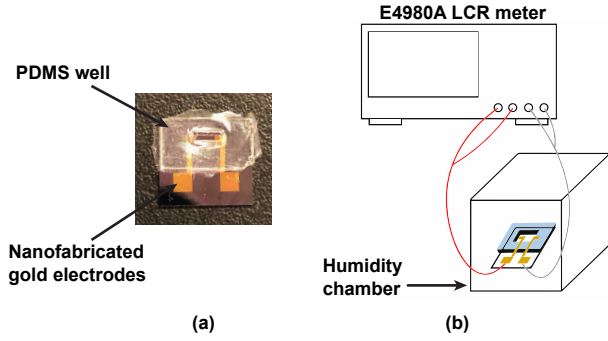
Fig. 2. Illustration of (a) electrode with a PDMS well and (b) experimental setup.

Fig. 3. Circuit models for (a) KCl salt solution (b) blood, blood clot and serum.

II. MATERIALS AND METHODS

A. Measurement Setup

The sensor comprises microfabricated gold (Au) electrodes on a silicon substrate, as shown in Fig. 2(a). In brief, a 100 nm thermal oxide was grown on an epitaxial silicon wafer, followed by a 1 μm SiO_2 deposited via a plasma-enhanced chemical vapor deposition to isolate the electrodes from the substrate. The wafer was spin-coated with photoresist, the electrodes defined with maskless lithography, and a film stack consisting of a 15 nm chromium adhesion layer and 600 nm Au was sputtered and lifted off. The sensor chips were diced (9×10 mm^2), each containing a pair of electrodes (1×1 mm^2), and bonded to a 6 mm thick polydimethylsiloxane (PDMS) well by treating them with ultraviolet ozone. The PDMS layer was formed using a Sylgard 184 silicone elastomer kit with a custom 3D-printed mold (FormLabs 3B) containing a $3 \times 5 \times 6$ mm^3 cutout to hold up to a 90 μL sample. A taller PDMS well (14 mm thickness) was used in experiments needing a larger sample volume.

The electrodes were connected to an impedance analyzer (Keysight E4980A) using BNC cables, test hooks, and wires soldered to the electrodes, as shown in Fig. 2(b). The sample's electrical impedance was measured across the electrodes with a 50-mV amplitude to prevent redox reactions with the salts dissolved in the sample [18]. The resulting current was measured with the same electrode pair. The cable's parasitic impedance was accounted for by performing open and short corrections before measurements. The impedance analyzer measured the sample impedance in the series resistance (R) and reactance (X) mode. The impedance was recorded at 10 points per decade logarithmically spaced from 20 Hz – 2 MHz. This technique is known as electrical impedance spectroscopy (EIS).

B. Circuit Models and Equivalent Circuit Fitting

Electrical circuit models for blood are described in the literature, along with initial estimates of the parameters [16]. The electrical circuit model for blood, blood clot, and serum extends the traditional three-element model for cell suspensions [22]. In the model shown in Fig. 3, R_p is the plasma resistance, R_i is the interior resistance of erythrocytes, and CPE_i models the cell membrane. A shunt capacitor, C_{liq}, is added to model the dielectric capacitance of blood's intra-cellular and extra-cellular fluid, which is mainly water. The addition of C_{liq} provides a better fit for frequencies above 1 MHz [23].
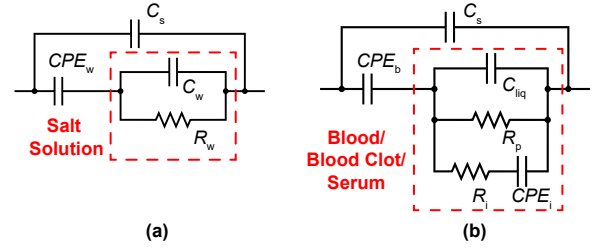
The measured EIS data was imported into ZView (Scribner Associates, Southern Pines, NC, USA) to fit the data to an equivalent circuit model. While fitting circuit models for the various samples, the electrode stray capacitance, C_s, was fixed (independent of the sample) to the measured value (described below), and the remaining model parameters were fit. Reducing the number of unknown parameters improves the fit and minimizes the chi-squared error. The sample impedance can then be extracted using the fitted electrical parameters. Accurate absolute conductivity measurements require accounting for the sample conductivity, the stray capacitance, C_s, and the cell constant, α.

C. Measuring Parasitic Impedances and the Cell Constant

Two important elements must be accounted for to avoid confounding measurements. Specifically, the electrodes have an inherent stray capacitance, C_s, due to the electric field coupling between the electrodes through the substrate and an impedance at the electrode-electrolyte interface due to the polarization of the electrodes [18]. In two-electrode measurement cells, the electrode polarization can be characterized using a constant phase element, CPE [23]. C_s is measured without the PDMS well attached to the electrodes and no sample. Since CPE depends on the sample placed in the well, it can be estimated by fitting EIS data with the equivalent circuit model of the sample and a CPE in series. The cell constant, α, depends on the electrode geometry and the cell's dimensions. Conventionally, α is defined as d/A for parallel-plate electrodes with perpendicular field lines, where d is the distance between the electrodes, and A is the electrode's cross-sectional area. However, estimating α using solutions with known conductivities is more appropriate for complex 3D geometries. EIS was performed on various potassium chloride (KCl) solutions (i.e., 0.01, 0.1, and 1 M) to calculate α. These solutions have known conductivities,

$$\sigma = \frac{d}{R_w A} = \frac{\alpha}{R_w} \tag{1}$$

where R_w is the solution resistance found by fitting the measured EIS data to the model shown in Fig. 3(a) [24]. The absolute conductivity of the samples was calculated by dividing α by the respective measured EIS resistance data, after de-embedding C_s and the electrode interface CPE_b, as shown in Fig. 3(b).

D. Blood Impedance Measurements

Porcine blood with a sodium citrate anticoagulant (1:9 anticoagulant to blood w/w ratio) was purchased from Lampire Biological Laboratories (#7204906) and stored at 4 °C. The
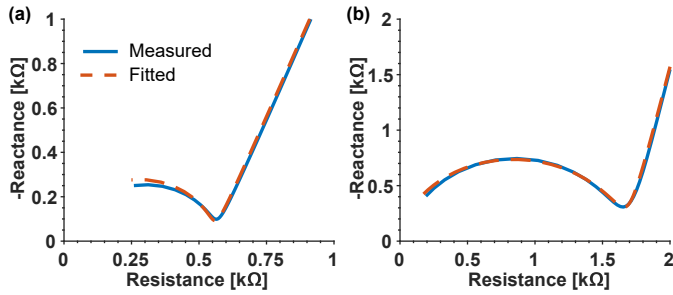
Fig. 4. Measured EIS spectra for (a) 0.1 M KCl solution and (b) blood.

TABLE I. FITTED CIRCUIT PARAMETERS (AVERAGE OF $N = 3$)

Parameter	Sample (C_s fixed at 144 pF)		
	Blood	Blood Clot	Serum
$CPE_b - Q$ (nS)	128	175	172
$CPE_b - n$	0.922	0.931	0.941
C_{liq} (pF)	~0	13.1	~0
R_p (kΩ)	1.68	2.17	0.547
R_i (kΩ)	1.24	~0	0.511
$CPE_i - Q$ (nS)	8.92	348	2,840
$CPE_i - n$	0.663	0.438	0.299

Fig. 5. (a) Nyquist plot; (b) Conductivity plot of blood, serum, and blood clot (n=3) after removing parasitic capacitance and the electrode polarization effect.

blood sample was equilibrated to room temperature (20 °C) for 30 min before every measurement. 80 µL blood samples were pipetted into the well. The electrodes were placed in a humidity chamber at room temperature to minimize the effect of blood drying [25]. The impedance analyzer was connected to a computer running a MATLAB script to acquire EIS data periodically. In blood coagulation experiments, 220 mM of calcium chloride (CaCl$_2$) was added in a volume ratio of 1:9 v/v to blood in a test tube to initiate the coagulation cascade [26]. The blood clot retracts slowly after coagulation, and the serum separates [17]. 30 min after initiating the coagulation cascade, the sample was centrifuged at 3,000 rpm for 5 min in an Eppendorf Centrifuge MiniSpin to separate the blood clot and serum phases more distinctively [27]. Next, the blood clot and serum were placed in the well separately, and the impedance was measured using EIS. In another experiment, blood samples (n=3) were used to measure the impedance variation when blood was clotted in the tall well by adding CaCl$_2$ solution.

III. MEASUREMENT RESULTS

A. Electrode Parameters and Equivalent Circuit Fitting

C_s was measured to be 144 pF, and α was calculated by measuring KCl conductivity (9 measurements using 3 separate electrodes and 3 KCl concentrations) for an average α of 732.35 m^{-1}. Subsequently, the established setup measured EIS spectra of blood, and the data fit with the circuit model depicted in Fig. 4. The circuit model incorporates a constant phase element rather than a conventional capacitor to model the erythrocyte membrane capacitance [22]. This approach minimized the chi-squared error, enhancing the fit of the circuit model.

B. Blood and Blood Clot Comparison

The coagulated blood in a test tube was centrifuged, and EIS was performed separately on the blood clot and serum in the well. The measured EIS data were fit to the circuit model shown
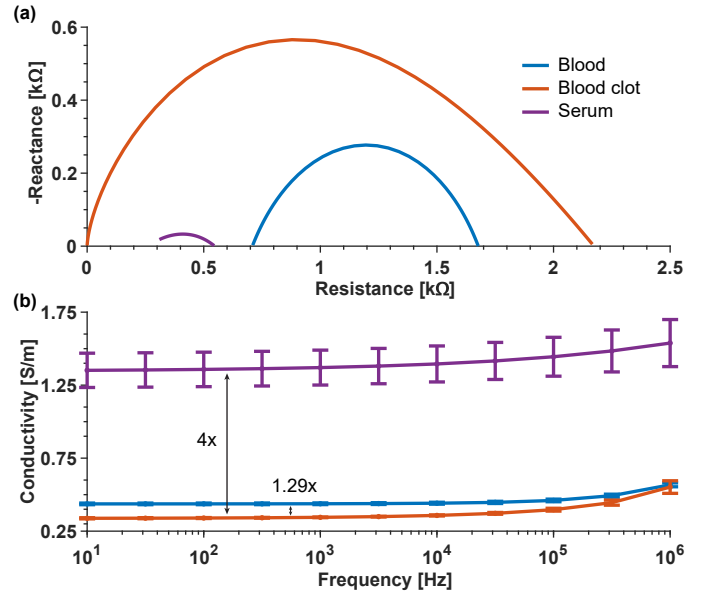
in Fig. 3(b), and the resulting coefficients are summarized in Table I. Figure 5 compares the Nyquist plots and absolute conductivity of the measured impedance of blood, blood clot, and serum from three separate trials. At frequencies below 100 kHz, the conductivity of blood is relatively constant since the current predominantly flows through the plasma [28]. The erythrocyte membrane's interfacial polarization at higher frequencies increases blood's conductivity [29]. The calculated conductivity of blood is 0.44 S/m, blood clot is 0.34 S/m, and serum is 1.50 S/m at 1 kHz. The conductivity of a porcine blood clot is ~25% lower than that of whole blood, up to 10 kHz.

C. Time Course Blood Impedance Change

Blood can be modeled as a homogenous suspension of erythrocytes in plasma [16]. The settling of a homogeneous suspension can be explained by the theory of sedimentation, which suggests the presence of approximately four distinct settling zones [16]. In the bottom settling zone, the erythrocytes start aggregating over the electrodes over time. This process is known as erythrocyte sedimentation. ESR is a common hematology test that can indicate inflammatory activity within the body [30]. Erythrocyte sedimentation over the electrodes increases the impedance of the blood sample. During testing, it was also observed that blood drying increases the impedance, and a humidity chamber was used to mitigate this confounding effect. Blood impedance measurements were performed inside and outside a humidity chamber at 2-minute intervals over 6 hours to characterize this effect. Figure 6 shows the Nyquist plots at 30-min intervals for readability, along with the variation of R_p over time. As illustrated in Fig. 3(b), the impedance of blood has two parallel branches, namely the erythrocytes (R_i and CPE_i) and the plasma (R_p). R_i and CPE_i are relatively constant, while R_p increases over time, signifying the growing dominance of the erythrocytes in the blood impedance [28]. After all the erythrocytes reach a stable state at the bottom of the well, the R_p stops increasing. When this measurement is performed outside the humidity chamber, the top surface of the blood starts to dry
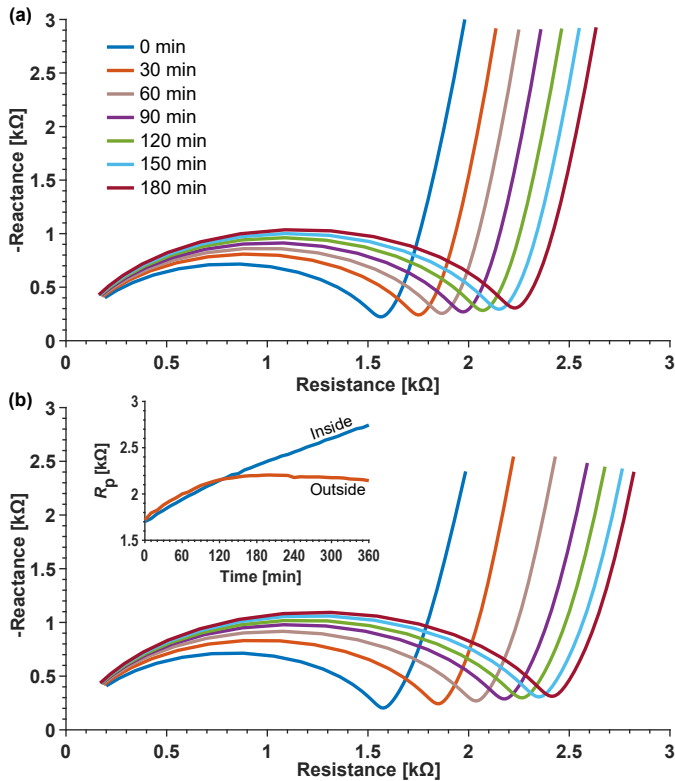
Fig. 6. Blood drying and sedimentation measured (a) inside a humidity chamber and (b) outside a humidity chamber. Inset shows R_p variation over time.

Fig. 7. Normalized impedance change at 10 kHz of blood (n=3) clotted in the well over time. Inset shows the variation of T_{clot} with CaCl$_2$ concentration.

TABLE II.   CONDUCTIVITY COMPARISON

Parameter	[15]	[17]	[18], [21]	[20]	*This work*
Blood species	Porcine	Human	Human	Human	Porcine
Anticoagulant	ACD	Citrate	PPACK	EDTA	Na Citrate
Test frequency (kHz)	1	10	300	1	1
Humidity control	No	Yes	No	No	Yes
Blood σ (S/m)	-	-	-	0.4	0.44
Clot σ (S/m)	-	-	-	-	0.34
Serum σ (S/m)	-	-	-	-	1.5
Conductivity ratio of blood and blood clot	1,000	1.28	1.16	-	1.29

due to evaporation. The evaporation process accelerates the sedimentation of erythrocytes by exerting an additional downward force [31]. It can be observed that R_p reaches a steady state after 2 hours in this case. When measurements are conducted with humidity control, R_p can serve as a proxy for measuring ESR (units are mm/hr) after appropriate calibration.

D. Variation of Impedance with Blood Clotting over Time

Figure 7 shows the variation of normalized impedance with time for blood clotting over 3 separate trials showing a plateau. The impedance reaches a peak value at a specific time, denoted as T_{clot}, which proved challenging to discern accurately in a few trials. This peak corresponds to the formation of the clot within the well and the subsequent retraction of serum over the electrodes. Initially, when the clot forms in the well, the serum is retracted over the electrodes, and there is a brief decrease in impedance. However, the clot settles down over the electrodes due to its higher density than serum, and the impedance rises again. Notably, Fig. 7 demonstrates that increasing the concentration of Ca^{2+} ions added to the blood reduces T_{clot}.

IV. DISCUSSION

In this study, the absolute conductivity of blood, blood clot, and serum samples were measured and compared with values reported in the literature in Table II. The conductivity ratio of blood and blood clot is concordant with previous studies, except for one outlier. Ref. [15] reports a 1,000x conductivity ratio, which others (and this work) have not reproduced. The lack of a humidity chamber likely contributed to this discrepancy, while other distinguishing factors are not discernible. It is important to consider the drying properties of blood, often overlooked in previous studies, as it can lead to inaccurate assessments of impedance and coagulation behavior. Rapid drying of blood within 30 minutes at room temperature has been reported. A humidity chamber or a similar technique should be employed to mitigate the drying effect, ensuring precise measurements and reliable characterization of blood coagulation.

Blood's time course impedance change outside a humidity chamber is similar to previous reports [16]. Moreover, the impedance phase plots of serum and blood clot, and T_{clot} are also consistent [17]. It is observed that blood with moderate conductivity separates into serum with higher conductivity (due to the lack of erythrocytes) and blood clots with lower conductivity. Serum is 4x, and blood is 1.29x as conductive as blood clots. After clotting, serum comprises approximately 55% of the volume. When operating with a few μL of blood, it may not be sufficient to form a clot large enough to cover the electrodes. Consequently, a significant volume of serum in the measurement chamber and coagulated blood can potentially influence the electrical impedance measurement.

This research paves the way for PoC applications and minimizes the need for extensive laboratory processing and reducing turn-around times. It lays the groundwork for further research and development to refine and validate the impedance-based approach for measuring ESR and T_{clot}. Furthermore, this impedance-based technique allows for analyzing material-blood interactions, facilitating the assessment of materials' thrombogenicity. This advancement can help develop innovative materials for cardiovascular prostheses that delay or prevent thrombosis formation [32], [33].

REFERENCES

[1] M. T. Ganter and C. K. Hofer, "Coagulation Monitoring: Current Techniques and Clinical Use of Viscoelastic Point-of-Care Coagulation Devices," *Anesthesia & Analgesia*, vol. 106, no. 5, pp. 1366–1375, May 2008, doi: 10.1213/ane.0b013e318168b367.

[2] J. A. Condrey *et al.*, "Prothrombin Time, Activated Partial Thromboplastin Time, and Fibrinogen Reference Intervals for Inbred Strain 13/N Guinea Pigs (Cavia porcellus) and Validation of Low Volume Sample Analysis," *Microorganisms*, vol. 8, no. 8, p. 1127, Jul. 2020, doi: 10.3390/microorganisms8081127.

[3] S. Casella, C. Giannetto, F. Fazio, E. Giudice, and G. Piccione, "Assessment of Prothrombin Time, Activated Partial Thromboplastin Time, and Fibrinogen Concentration on Equine Plasma Samples following Different Storage Conditions," *J VET Diagn Invest*, vol. 21, no. 5, pp. 674–678, Sep. 2009, doi: 10.1177/104063870902100512.

[4] Y. Chee, "Coagulation," *J R Coll Physicians Edinb*, vol. 44, no. 1, pp. 42–45, 2014, doi: 10.4997/JRCPE.2014.110.

[5] T. Cohen, T. Haas, and M. M. Cushing, "The strengths and weaknesses of viscoelastic testing compared to traditional coagulation testing," *Transfusion*, vol. 60, no. S6, Oct. 2020, doi: 10.1111/trf.16073.

[6] D. Maji *et al.*, "ClotChip: A Microfluidic Dielectric Sensor for Point-of-Care Assessment of Hemostasis," *IEEE Trans. Biomed. Circuits Syst.*, vol. 11, no. 6, pp. 1459–1469, Dec. 2017, doi: 10.1109/TBCAS.2017.2739724.

[7] W. Xu, J. Appel, and J. Chae, "Real-Time Monitoring of Whole Blood Coagulation Using a Microfabricated Contour-Mode Film Bulk Acoustic Resonator," *J. Microelectromech. Syst.*, vol. 21, no. 2, pp. 302–307, Apr. 2012, doi: 10.1109/JMEMS.2011.2179011.

[8] L. Müller *et al.*, "Investigation of Prothrombin Time in Human Whole-Blood Samples with a Quartz Crystal Biosensor," *Anal. Chem.*, vol. 82, no. 2, pp. 658–663, Jan. 2010, doi: 10.1021/ac9021117.

[9] L. G. Puckett, J. K. Lewis, A. Urbas, X. Cui, D. Gao, and L. G. Bachas, "Magnetoelastic transducers for monitoring coagulation, clot inhibition, and fibrinolysis," *Biosensors and Bioelectronics*, vol. 20, no. 9, pp. 1737–1743, Mar. 2005, doi: 10.1016/j.bios.2004.06.051.

[10] G. P. Carpenter, T. G. Neel, and J. R. Parker, "Overview of a novel point of care instrument system for measuring whole blood Prothrombin time," presented at the OE/LASE '94, R. F. Bonner, G. E. Cohn, T. M. Laue, and A. V. Priezzhev, Eds., Los Angeles, CA, Jul. 1994, pp. 205–213. doi: 10.1117/12.180788.

[11] C.-C. Huang and S.-H. Wang, "Characterization of Blood Properties from Coagulating Blood of Different Hematocrits Using Ultrasonic Backscatter and Attenuation," *Jpn. J. Appl. Phys.*, vol. 45, no. 9A, pp. 7191–7196, Sep. 2006, doi: 10.1143/JJAP.45.7191.

[12] M. Andersson, J. Andersson, A. Sellborn, M. Berglin, B. Nilsson, and H. Elwing, "Quartz crystal microbalance-with dissipation monitoring (QCM-D) for real time measurements of blood coagulation density and immune complement activation on artificial surfaces," *Biosensors and Bioelectronics*, vol. 21, no. 1, pp. 79–86, Jul. 2005, doi: 10.1016/j.bios.2004.09.026.

[13] A. Ur, "Changes in the Electrical Impedance of Blood during Coagulation," *Nature*, vol. 226, no. 5242, pp. 269–270, Apr. 1970, doi: 10.1038/226269a0.

[14] A. Ur, "Analysis and Interpretation of the Impedance Blood Coagulation Curve," *Am J Clin Pathol*, vol. 67, no. 5, pp. 470–476, May 1977, doi: 10.1093/ajcp/67.5.470.

[15] K. F. Lei, K.-H. Chen, P.-H. Tsui, and N.-M. Tsang, "Real-Time Electrical Impedimetric Monitoring of Blood Coagulation Process under Temperature and Hematocrit Variations Conducted in a Microfluidic Chip," *PLoS ONE*, vol. 8, no. 10, p. e76243, Oct. 2013, doi: 10.1371/journal.pone.0076243.

[16] A. Zhbanov and S. Yang, "Electrochemical impedance spectroscopy of blood for sensitive detection of blood hematocrit, sedimentation and dielectric properties," *Anal. Methods*, vol. 9, no. 22, pp. 3302–3313, 2017, doi: 10.1039/C7AY00714K.

[17] G. D'Ambrogio *et al.*, "Investigation of Blood Coagulation Using Impedance Spectroscopy: Toward Innovative Biomarkers to Assess Fibrinogenesis and Clot Retraction," *Biomedicines*, vol. 10, no. 8, p. 1833, Jul. 2022, doi: 10.3390/biomedicines10081833.

[18] A. Affanni, G. Chiorboli, R. Specogna, and F. Trevisan, "Uncertainty model of electro-optical thrombus growth estimation for early risk detection," *Measurement*, vol. 79, pp. 260–266, Feb. 2016, doi: 10.1016/j.measurement.2015.05.045.

[19] Y. Asakura, A. Sapkota, O. Maruyama, R. Kosaka, T. Yamane, and M. Takei, "Relative permittivity measurement during the thrombus formation process using the dielectric relaxation method for various hematocrit values," *J Artif Organs*, vol. 18, no. 4, pp. 346–353, Dec. 2015, doi: 10.1007/s10047-015-0847-8.

[20] N. Istuk, A. L. Gioia, H. Benchakroun, A. Lowery, B. McDermott, and M. O'Halloran, "Relationship Between the Conductivity of Human Blood and Blood Counts," *IEEE J. Electromagn. RF Microw. Med. Biol.*, vol. 6, no. 2, pp. 184–190, Jun. 2022, doi: 10.1109/JERM.2021.3130788.

[21] D. De Zanet *et al.*, "Impedance biosensor for real-time monitoring and prediction of thrombotic individual profile in flowing blood," *PLoS ONE*, vol. 12, no. 9, p. e0184941, Sep. 2017, doi: 10.1371/journal.pone.0184941.

[22] Y. Ulgen and M. Sezdi, "Electrical parameters of human blood," in *Proceedings of the 20th Annual International Conference of the IEEE Engineering in Medicine and Biology Society. Vol.20 Biomedical Engineering Towards the Year 2000 and Beyond (Cat. No.98CH36286)*, Hong Kong, China: IEEE, 1998, pp. 2983–2986. doi: 10.1109/IEMBS.1998.746117.

[23] Z. Chang, G. A. M. Pop, and G. C. M. Meijer, "A Comparison of Two- and Four-Electrode Techniques to Characterize Blood Impedance for the Frequency Range of 100 Hz to 100 MHz," *IEEE Trans. Biomed. Eng.*, vol. 55, no. 3, pp. 1247–1249, Mar. 2008, doi: 10.1109/TBME.2008.915725.

[24] Y. C. Wu, W. F. Koch, and K. W. Pratt, "Proposed new electrolytic conductivity primary standards for KCl solutions," *J. RES. NATL. INST. STAN.*, vol. 96, no. 2, p. 191, Mar. 1991, doi: 10.6028/jres.096.008.

[25] F. Ramsthaler, P. Schmidt, R. Bux, S. Potente, C. Kaiser, and M. Kettner, "Drying properties of bloodstains on common indoor surfaces," *Int J Legal Med*, vol. 126, no. 5, pp. 739–746, Sep. 2012, doi: 10.1007/s00414-012-0734-2.

[26] K. Wood *et al.*, "In Vitro Blood Clot Formation and Dissolution for Testing New Stroke-Treatment Devices," *Biomedicines*, vol. 10, no. 8, p. 1870, Aug. 2022, doi: 10.3390/biomedicines10081870.

[27] J. Cadamuro *et al.*, "Influence of centrifugation conditions on the results of 77 routine clinical chemistry analytes using standard vacuum blood collection tubes and the new BD-Barricor tubes," *Biochemia Medica*, vol. 28, no. 1, p. 010704, Feb. 2018, doi: 10.11613/BM.2018.010704.

[28] T.-X. Zhao, B. Jacobson, and T. Ribbe, "Triple-frequency method for measuring blood impedance," *Physiol. Meas.*, vol. 14, no. 2, pp. 145–156, May 1993, doi: 10.1088/0967-3334/14/2/006.

[29] F. Bordi, C. Cametti, and T. Gili, "Dielectric spectroscopy of erythrocyte cell suspensions. A comparison between Looyenga and Maxwell–Wagner–Hanai effective medium theory formulations," *Journal of Non-Crystalline Solids*, vol. 305, no. 1–3, pp. 278–284, Jul. 2002, doi: 10.1016/S0022-3093(02)01111-0.

[30] K. Tishkowski and V. Gupta, "Erythrocyte Sedimentation Rate," *StatPearls*, Apr. 2023, [Online]. Available: https://www.ncbi.nlm.nih.gov/books/NBK557485/

[31] J. Y. Kim, M. Gonçalves, N. Jung, H. Kim, and B. M. Weon, "Evaporation and deposition of inclined colloidal droplets," *Sci Rep*, vol. 11, no. 1, p. 17784, Sep. 2021, doi: 10.1038/s41598-021-97256-w.

[32] X. Wang *et al.*, "Improvement of blood compatibility of artificial heart valves via titanium oxide film coated on low temperature isotropic carbon," *Surface and Coatings Technology*, vol. 128–129, pp. 36–42, Jun. 2000, doi: 10.1016/S0257-8972(00)00659-9.

[33] M. Behbahani *et al.*, "A review of computational fluid dynamics analysis of blood pumps," *Eur. J. Appl. Math*, vol. 20, no. 4, pp. 363–397, Aug. 2009, doi: 10.1017/S0956792509007839.